PAEDIATRIC NEURORADIOLOGY

Relative cerebral blood volume from dynamic susceptibility contrast perfusion in the grading of pediatric primary brain tumors

Chang Y. Ho · Jeremy S. Cardinal · Aaron P. Kamer · Stephen F. Kralik

Abstract

Introduction The aim of this study is to evaluate the utility of relative cerebral blood volume (rCBV) data from dynamic susceptibility contrast (DSC) perfusion in grading pediatric primary brain tumors.

Methods A retrospective blinded review of 63 pediatric brain tumors with DSC perfusion was performed independently by two neuroradiologists. A diagnosis of low- versus high-grade tumor was obtained from conventional imaging alone. Maximum rCBV (rCBVmax) was measured from manual ROI placement for each reviewer and averaged. Whole-tumor CBV data was obtained from a semi-automated approach. Results from all three analyses were compared to WHO grade.

Results Based on conventional MRI, the two reviewers had a concordance rate of 81 % ($k=0.62$). Compared to WHO grade, the concordant cases accurately diagnosed high versus low grade in 82 %. A positive correlation was demonstrated between manual rCBVmax and tumor grade ($r=0.30$, $P=0.015$). ROC analysis of rCBVmax (area under curve 0.65, 0.52–0.77, $P=0.03$) gave a low-high threshold of 1.38 with sensitivity of 92 % (74–99 %), specificity of 40 % (24–57 %), NPV of 88 % (62–98 %), and PPV of 50 % (35–65 %) Using this threshold on 12 discordant tumors between evaluators from conventional imaging yielded correct diagnoses in nine patients. Semi-automated analysis demonstrated statistically significant differences between low- and high-grade tumors for multiple metrics including average rCBV ($P=0.027$).

Conclusions Despite significant positive correlation with tumor grade, rCBV from pediatric brain tumors demonstrates limited specificity, but high NPV in excluding high-grade neoplasms. In selective patients whose conventional imaging is nonspecific, an rCBV threshold may have further diagnostic value.

Keywords Dynamic susceptibility contrast perfusion · Relative cerebral blood volume · World Health Organization tumor grading · Primary pediatric brain tumors

Introduction

Dynamic susceptibility contrast (DSC) perfusion MRI has demonstrated utility in the pretreatment evaluation of adult intracranial neoplasms for tumor grading, guiding biopsy, and prognosis [1–7]. While DSC perfusion MRI research for the assessment of adult brain tumors has grown substantially in the past 15 years, far less data exists regarding pediatric brain tumors. We evaluate the utility of DSC perfusion in differentiating low-grade versus high-grade tumors using both a manual and semi-automated method compared to the grading obtained from conventional MR images.

Materials and methods

Following institutional review board approval, a retrospective radiology database search from September 2009 to August 2013 was performed for pediatric brain tumor patients with pathology-proven diagnoses and World Health Organization (WHO) grade who had DSC perfusion MRI on initial evaluation prior to any surgical intervention, radiation, or chemotherapy. Patients who were treated with dexamethasone prior to MRI were not excluded from the study.

C. Y. Ho (✉) · J. S. Cardinal · A. P. Kamer · S. F. Kralik
Department of Radiology, MRI Department, Indiana University
School of Medicine, 705 Riley Hospital Drive, Indianapolis,
IN 46202, USA
e-mail: cyho@iupui.edu

MR imaging

DSC perfusion MR images were obtained during the first pass of a bolus of gadobenate dimeglumine (MultiHance, Bracco Diagnostics Inc., Princeton, NJ) on 1.5 and 3T MRI scanners (Siemens Avanto and Verio, Erlangen, Germany) using a gradient echo EPI sequence (TR 1410–2250/TE 30–45 ms, flip angle 90°). A contrast medium dose of 0.1 mmol/kg of body weight was injected followed by a normal saline flush for a total volume of 32 ml. When possible, an 18- or 20-gauge peripheral intravenous access was used with a power injector rate of 5 ml/s. In some cases, primarily with smaller children, only 24-gauge peripheral intravenous access was possible, limiting contrast injection rate and quality of the contrast bolus. Contrast bolus adequacy was evaluated by two fellowship-trained board-certified neuroradiologists (C. H. with 7 years experience and S. K. with 3 years experience) with certificate of added qualification based on time to signal intensity curves and included or excluded in consensus.

Qualitative analysis

The two reviewers (C.H. and S.K.) independently reviewed the conventional MR images including T1-weighted, T2-weighted, T2 FLAIR, DWI, and post-contrast T1-weighted series, blinded to DSC perfusion data and pathological diagnosis and individually graded the tumors as low or high grade. Interobserver agreement for conventional MR assessment was performed and compared to final pathological outcome.

Manual analysis of tumor rCBV maximum

Quantitative analysis of tumor relative cerebral blood volume (rCBV) was performed by two neuroradiologists (C.H. and S.K.) using a commercially available workstation (DynaSuite Neuro 3.0 workstation, InVivo Corp, Pewaukee WI). Each neuroradiologist independently obtained a rCBV maximum (rCBVmax) for each tumor by drawing at least three 2–5 mm^2 ROIs within the perceived highest CBV within tumor tissue and using the highest value divided by a similar ROI placed in normal-appearing contralateral white matter (Fig. 1). Conventional MR images were available to assist in ROI placement within the tumor and avoid placement within a vessel. Workstation-generated corrected CBV maps were used, with CBV correction by gamma variate fitting and an algorithm developed by Boxerman et al. [8]. The tumor rCBVmax value used for grading was then generated by averaging the maximum values obtained by the two neuroradiologists for each tumor and was correlated to histologic WHO grade with Spearman's rho. Receiver operating characteristic (ROC) analyses and Youden's index were performed to determine the optimum tumor rCBVmax threshold for tumor grading.

Semi-automated analysis of whole-tumor rCBV

Semi-automated rCBV calculation was performed for each tumor using an in-house script (MATLAB R2011b, The Mathworks, Inc., Natick, Massachusetts). Freehand ROIs were placed by a board-certified neuroradiologist (A.K.) with certificate of added qualification outlining the entire tumor on axial CBV maps generated from the MRI scanner (Syngo Neuro Perfusion, Siemens Healthcare, Erlangen, Germany). Pre and post-contrast T1-weighted, T2-weighted, and T2 FLAIR images were concurrently used to define the margins of the tumor and avoid large blood vessels and cystic areas within the ROI. Additionally, a small ROI was placed in normal-appearing white matter. For each voxel within the tumor ROI, an rCBV value was automatically calculated by dividing the tumor CBV voxel value by the mean CBV value of normal-appearing white matter. rCBV voxel values for each tumor were exported to comma-separated value (CSV) files for import to Microsoft Excel 2010. Two tumors (one low-grade and one high-grade tumor) were not able to be processed using the in-house script because of susceptibility artifact on the CBV maps. These two tumors were excluded from the whole-tumor rCBV analysis. Individual histograms were generated for the whole-tumor rCBV voxel data. rCBV bin widths of 0.1 were chosen based on the trade-off between detail and noise within the histograms. Statistical metrics calculated for the rCBV data for each tumor included mean, standard deviation, skew, kurtosis, peak height, peak location, and multiple percentiles (5th, 10th, 25th, 50th, 75th, 90th, and 95th). Means and standard deviations were calculated for each metric, grouped by low- and high-grade tumor. Statistical significance of the low- and high-grade means were calculated using the unpaired, two-tailed Student's t test Additionally, Spearman's rho correlation was performed between the semi-automated whole-tumor rCBV data and the manually obtained tumor rCBVmax values.

Statistical software

Statistical analysis was performed using Microsoft Excel 2010, SPSS 21 (IBM Corp. Armonk, NY), and an online statistical calculator (Vassarstats, http://vassarstats.net/).

Pathology

Histopathologic evaluation of surgical specimens for all tumors was performed by one of two board-certified neuropathologists who determined a diagnosis and assigned a WHO grade of I through IV. For the purposes of this study, WHO grades I and II tumors are considered low grade and WHO grades III and IV tumors are considered high grade.

Fig. 1 Axial **a** T1-weighted post-contrast and **b** CBV map in a 5-year-old male with pilomyxoid astrocytoma. ROIs are placed within the tumor at the site of perceived highest CBV and in the normal-appearing cerebellar white matter
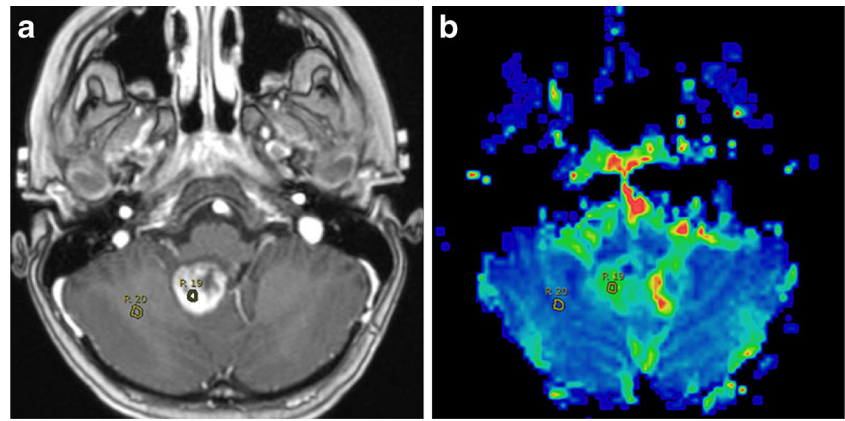
Effect of dexamethasone on rCBVmax

Analysis of an electronic patient database was performed for the presence and timing of dexamethasone treatment in relation to the pretreatment DSC MRI. Student's *t* test was performed to evaluate for any significant differences in rCBVmax between all tumors, between all grade I tumors, between all grade IV tumors, between medulloblastomas, and between pilocytic astrocytomas treated with dexamethasone versus without.

Results

A total of 65 cases were found matching inclusion criteria. Two cases were excluded due to nondiagnostic DSC data for a total of 63 cases for review. One case was excluded for poor contrast bolus and the second for significant susceptibility artifact generated by the patient's dental braces. Patient clinical data is summarized in Table 1. The mean age of the patients was 6.3 years (range, 1.0–16.8 years, 39 male, 24 female). Thirty-eight tumors were low grade, and 25 tumors were high grade Thirty-nine tumors were infratentorial and 24 tumors were supratentorial.

Qualitative analysis of tumor grade

Based on conventional MR images, one reviewer (C. H.) correctly assessed low versus high grade in 81 % (51/63) of patients (29 of 38 low-grade tumors and 22 of 25 high-grade tumors) for a sensitivity of 88 % (95CI, 68–97 %), specificity of 76 % (95CI, 59–88 %), positive predictive value (PPV) of 71 % (95CI, 52–85 %), and negative predictive value (NPV) of 91 % (95CI, 74–98 %). The other reviewer (S. K.) correctly assessed low versus high grade in 71 % (45/63) of patients (31 of 38 low-grade tumors and 14 of 25 high-grade tumors) for a sensitivity of 56 % (95CI, 35–75 %), specificity of 82 % (95CI, 65–92 %), PPV of 67 % (95CI, 43–85 %), and NPV of 74 % (95CI, 58–86 %).

The two observers agreed on tumor grade based on conventional MR imaging in 51 of 63 (81 %) cases (36 of 38 low grade and 15 of 25 high-grade tumors), resulting in a Cohen's kappa of 0.62 (95 % CI, 0.42–0.82). Forty-two of these concordant diagnoses matched pathologic results giving an accuracy rate of 82 % for a sensitivity of 87 % (95CI, 58–98 %), specificity of 81 % (95CI, 63–91 %), PPV of 65 % (95CI, 41–84 %), and NPV of 94 % (95CI, 78–99 %).

Manual analysis of tumor rCBV maximum

Manual rCBV data is summarized in Table 1 and graphically represented in Fig. 2. Tumor rCBVmax demonstrated significant positive correlation with tumor grade (Spearman's rho, 0.30; $P=.015$). ROC analysis of tumor rCBVmax to predict high-grade tumor demonstrated an area under the curve of 0.65 (95CI, 0.52–0.77, $P=0.03$) (Fig. 3). A tumor rCBV cutoff value of 1.38 was selected by maximizing Youden's index, which resulted in a sensitivity of 92 % (95CI, 74–99 %), specificity of 40 % (95CI, 24–57 %), PPV of 50 % (95CI, 35–65 %), and NPV of 88 % (95CI, 62–98 %). Results were similar when tumors were grouped by infratentorial and supratentorial locations. For infratentorial tumors, an rCBV cutoff of 1.38 resulted in a sensitivity of 89 % (95CI, 65–98 %), specificity of 40 % (95CI, 20–64 %), PPV of 59 % (95CI, 39–76 %), and NPV of 80 % (95CI, 44–96 %). For supratentorial tumors, an rCBV cutoff of 1.38 resulted in a sensitivity of 100 % (95CI, 52–100 %), specificity of 39 % (95CI, 18–64 %), PPV of 35 % (95CI, 15–61 %), and NPV of 100 % (95CI, 56–100 %). In reassessing the 12 discordant cases between reviewers from conventional imaging alone, which could be considered challenging for pediatric neuroradiologists from a diagnostic standpoint, utilizing the manual rCBVmax threshold of 1.38 resulted in an accurate diagnosis of high- versus low-grade tumor in another 9 cases (75 %).

Semi-automated analysis of whole-tumor rCBV

Semi-automated rCBV data is summarized in Table 2. Statistically significant differences were demonstrated

Table 1 Patient characteristics and tumor manual rCBVmax data

	Cases	Sex		Age		rCBVmax
		M	F	Average	Range	Average±Std Dev
All cases	63	39	24	6.3	1.0–16.8	3.7±3.1
Posterior fossa	39	25	14	5.6	1.2–14.2	3.8±2.8
Supratentorial	24	14	10	7.4	1.0–16.8	3.6±3.4
WHO I	25	14	11	7.1	1.1–15.0	2.9±2.5
WHO II	13	5	8	5.9	1.2–16.8	4.0±3.7
WHO III	9	8	1	4.6	1.4–12.0	2.9±1.8
WHO IV	16	12	4	6.4	1.0–16.2	5.1±3.2
Pilocytic astrocytoma	17	9	8	7.3	2.2–15.0	3.3±2.8
Medulloblastoma	9	6	3	6.8	2.3–13.3	3.8±1.7
Ependymoma WHO III	7	7	0	4.3	1.4–12.0	3.1±2.0
Pilomyxoid astrocytoma	6	3	3	2.9	1.2–5.8	3.5±4.3
Ependymoma WHO II	3	0	3	2.2	1.5–2.9	6.6±2.2
ATRT	3	2	1	1.4	1.0–1.9	6.9±0.8
GBM	3	3	0	6.9	4.2–9.5	3.9±1.7
Choroid plexus papilloma	2	2	0	4.1	3.1–5.2	3.8±1.4
Fibrillary astrocytoma	1	0	1	4.3		0.5
Craniophayngioma	1	0	1	5.5		0.7
Desmoplastic infantile ganglioglioma	1	0	1	1.1		2.6
Ganglioglioma	1	1	0	12.9		2.4
Ganglion cell tumor	1	0	1	1.8		0.9
High-grade diffuse glioma	1	0	1	6.9		1.4
Low-grade glioma	1	1	0	12.8		2.8
Low-grade glioneuronal tumor	1	1	0	11.5		0.9
Low-grade oligoastrocytoma	1	0	1	16.8		1.1
Oligodendroglioma	1	1	0	15.5		2.1
Pineal parenchymal tumor WHO II	1	1	0	15.6		7.1
Supratentorial PNET	1	1	0	16.2		15.2
Anaplastic astrocytoma	1	1	0	4		3.6

between low-grade and high-grade tumors for whole-tumor average rCBV ($P=.027$), peak location ($P=.011$), and several measured percentiles with 25th percentile showing the strongest statistical significance ($P=.013$). Whole-tumor 95th percentile rCBV correlated with tumor rCBVmax obtained by manual ROI (Spearman's rho, 0.64; $P<.001$).

Subjective analysis of whole-tumor rCBV histogram data showed a trend toward broader, more irregular histogram curves, and higher overall rCBV values with higher tumor grade; however, overlap existed between the low- and high-grade tumor groups (Fig. 4).

Effect of dexamethasone on rCBVmax

Sixty-five percent of included patients were emergently treated with dexamethasone prior to DSC MRI, with 100 % of dexamethasone treatment initiated within 2 days of DSC MRI. There was no significant difference in the rCBVmax values between all tumors ($P=0.19$), between all WHO grade I tumors ($P=0.63$), between all WHO grade IV tumors ($P=0.40$), between medulloblastomas ($P=0.82$), or between pilocytic astrocytomas ($P=0.11$) with and without dexamethasone treatment.

Discussion

The role of perfusion imaging in the diagnosis and management of pediatric brain tumor patients has not been clearly established, particularly when compared to perfusion imaging in adult brain tumor patients. We analyzed the largest known series of pediatric brain tumors with DSC perfusion to further

Fig. 2 *Box* and *whisker* plot demonstrating range, 2nd quartile, 3rd quartile, and median values for tumor rCBV maximum obtained by manual ROI placement grouped by tumor grade and common pediatric tumor types. (*PA* pilocytic astrocytoma, *PMA* pilomyxoid astrocytoma, *Epend 2* ependymoma WHO grade II, *Epend 3* ependymoma WHO grade III, *MED* medulloblastoma.)
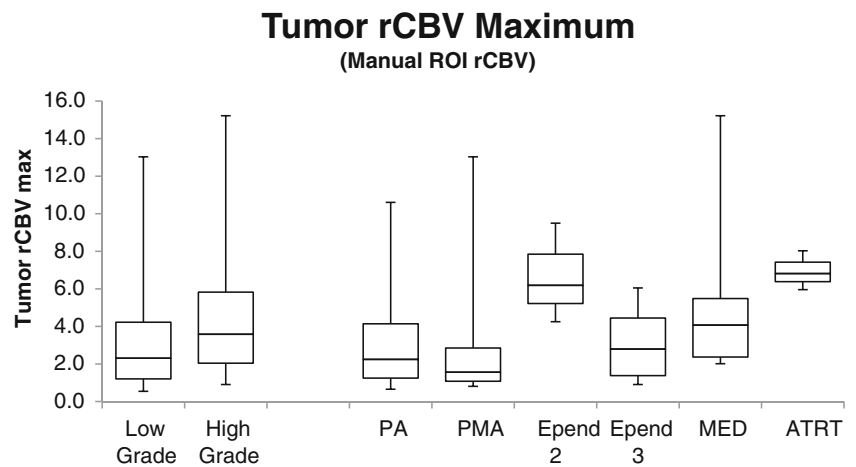
investigate the correlation between tumor perfusion characteristics and tumor grade. Ball and Holland [9] reviewed a large series of pediatric patients with DSC perfusion MRI performed for various indications, not only brain tumors, but did not find DSC perfusion useful in the evaluation of primary brain neoplasms, noting that benign tumors such as pilocytic astrocytomas may demonstrate flow similar to aggressive tumors such as medulloblastoma. Yeom et al. [10] recently reported a series of 54 pediatric brain tumors evaluated with arterial spin-labeling (ASL) perfusion MRI and showed that maximum relative tumor blood flow (rTBF) can be used to distinguish high-grade and low-grade tumors. rTBF obtained from ASL perfusion MRI in that study performed better than rCBV derived from DSC perfusion MRI in our study for classifying pediatric brain tumors as high or low grade. A notable difference in the results was better correlation of low rTBF with low-grade tumor compared to poor correlation of low rCBV with low-grade tumor. Similar to these studies, we

found a maximum tumor rCBV obtained by manual ROI demonstrated a significant positive correlation with pediatric brain tumor grade; however, the magnitude of correlation was low.

Considerable overlap exists between tumor rCBVmax values from the low-grade and high-grade pediatric brain tumors, compared to more consistently low rCBV demonstrated in low-grade adult glial tumors [1–7]. The most common low-grade tumors in our series whose rCBV overlapped with high-grade tumors were pilocytic astrocytomas and pilomyxoid astrocytomas. Pilocytic astrocytomas are described histologically as highly vascular tumors, frequently with markedly hyalinized and glomeruloid vessels which may mimic features of high-grade astrocytomas [11]. Pilomyxoid astrocytomas are closely related to pilocytic astrocytomas with some distinct characteristics and more aggressive behavior [12]. The high vascularity of these low-grade pediatric tumors likely results in the sometimes high tumor rCBVmax, which undermines the specificity of high rCBV for high-grade tumor. Similarly, an exception in the adult population is the well-documented elevated rCBV found in oligodendrogliomas, which has been

Table 2 Metrics for semi-automated whole-tumor rCBV analysis

	Low grade Avg±Std dev	High grade Avg±Std dev	P value
Average	0.99±0.53	1.48±0.95	*0.027*
Standard deviation	0.71±0.40	0.91±0.53	0.128
Skew	1.78±1.38	1.57±0.98	0.486
Kurtosis	8.33±14.69	5.20±7.11	0.271
Peak location	0.56±0.45	1.15±1.00	*0.011*
Peak height (normalized)	0.13±0.07	0.12±0.13	0.503
5th percentile	0.19±0.18	0.35±0.34	*0.042*
10th percentile	0.27±0.22	0.53±0.46	*0.017*
25th percentile	0.48±0.31	0.86±0.65	*0.013*
50th percentile	0.83±0.48	1.34±0.91	*0.018*
75th percentile	1.32±0.75	1.91±1.21	*0.038*
90th percentile	1.88±1.04	2.58±1.56	0.060
95th percentile	2.27±1.25	3.10±1.83	0.061

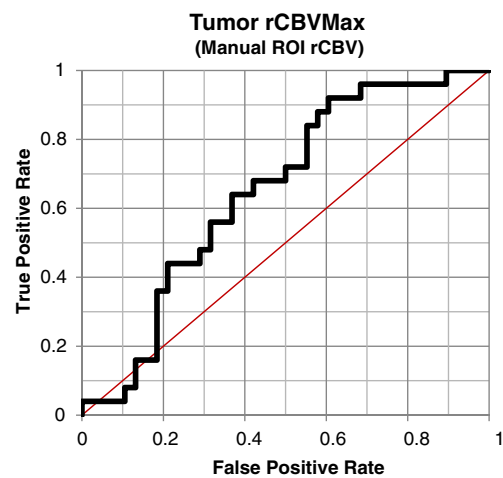Significant metrics are set in italics

Fig. 3 ROC analysis for tumor rCBV maximum obtained by manual ROI for predicting high-grade tumor

Fig. 4 Representative whole-tumor rCBV histograms. **a** pilocytic astrocytomas, **b** pilomyxoid astrocytomas, **c** ependymomas WHO grade II, **d** ependymomas WHO grade III, **e** medulloblastomas, and **f** ATRT. The *vertical axis* represents frequency, and the *horizontal axis* represents rCBV bin. Histograms were selected for each tumor type by choosing tumors with average rCBV closest to the tumor type group average, tumor type average minus 1 standard deviation, and tumor type average plus 1 standard deviation to give a representative sample
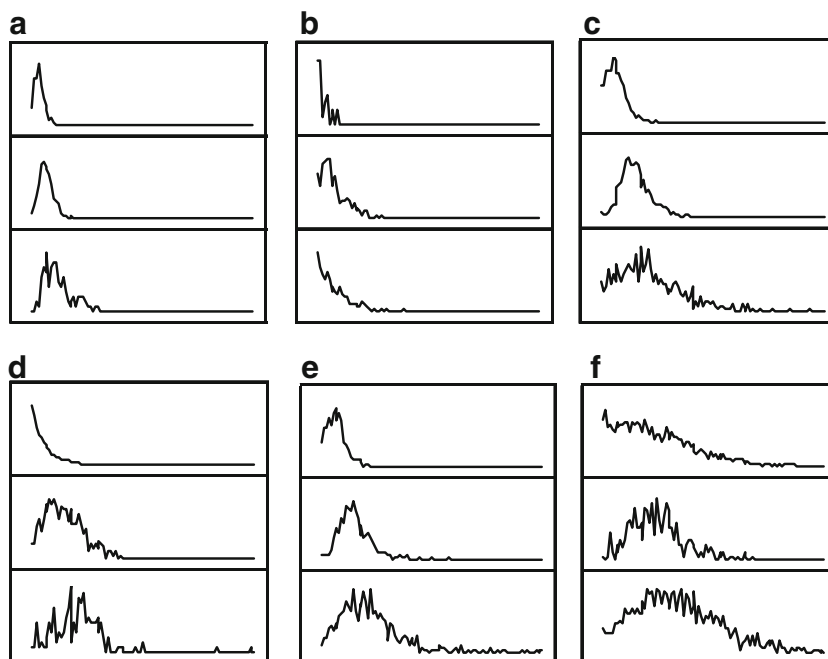
attributed to the high vascularity of these tumors [13, 14]. Conversely, maximum tumor rCBV was consistently elevated in the high-grade tumors in our series (medulloblastomas, atypical teratoid rhabdoid tumor (ATRT), WHO grade III ependymomas, and glioblastoma multiformes) similar to findings in adult high-grade tumors [1–7]. While a high tumor rCBVmax appears to have limited diagnostic value, a low rCBVmax may have value among pediatric brain tumors as a tool to exclude high-grade tumor, as demonstrated by our NPV of 88 % for all tumors in our series, rising to 100 % for supratentorial tumors using the rCBVmax cutoff of 1.38. rCBV thresholds have a better performance in adult intra-axial primary brain tumors due to the majority being WHO grades II–IV astrocytic tumors [1]. The majority of pediatric tumors are pilocytic astrocytomas and medulloblastomas, which is reflected by our patient population. We demonstrate a similar broad range and mean of rCBVmax values between these tumors, highlighting the difficulty of distinguishing between low- and high-grade tumors in the pediatric population from rCBVmax alone. Ultimately, the heterogeneity even within a single tumor diagnosis may reflect different genetic/molecular expressions, which have been described within medulloblastomas and have been shown to affect outcome [15]. rCBV differences within a single tumor diagnosis may eventually help distinguish these different molecular expressions.

Beyond the imaging differentiation of low-grade from high-grade pediatric brain tumors, determination of specific pediatric brain tumor pathology remains challenging with routine MRI sequences. Although our rCBVmax shows potential in differentiating ATRT (6.9±0.8) from medulloblastoma (3.8±1.7) (t=2.98, P=0.01), as demonstrated in Table 1,

insufficient data or overlap in tumor rCBVmax exists in other specific tumor pathologies.

A current limitation of the literature for determining rCBV trends for specific pediatric brain tumor pathologies is the considerable variability in rCBV values reported for these tumors. Cha [16] reported that pilocytic astrocytomas have moderately elevated rCBV while medulloblastomas have only mildly elevated rCBV. This is in contrast to our study in which pilocytic astrocytomas demonstrated mildly lower average tumor rCBVmax than medulloblastomas. However, pilocytic astrocytomas in our study demonstrated a wide range of tumor rCBVmax (0.65–10.6). Grand et al. [17] reported a series of nine pilocytic astrocytomas which demonstrated low rCBV (range 0.6–1.2). These reported rCBV values are both much lower and demonstrate much lower variability than the pilocytic astrocytomas in our study. Yuh et al. [18] reported that in their experience, ependymomas demonstrate markedly elevated rCBV. Our data supports this assertion with an average rCBVmax of 6.6 for WHO grade II ependymomas and 3.1 for WHO grade III ependymomas. Sentürk et al. [19] reported a series of intracranial tumors evaluated with DSC perfusion MRI with elevated rCBV demonstrated in both pilocytic astrocytomas and medulloblastomas/PNET similar to our data. The reason for discrepant results may be attributable to differences in DSC perfusion technical parameters, software analysis, and method of analysis including the subjective ROI placement. For example, differences in technique reported for the study performed by Grand et al. and our study include a flip angle of 45° compared to 90° and a larger rCBV ROI ranging from 30 to 150 mm^2 compared to 3–5 mm^2 in our study. Because there is currently no formally recognized DSC MRI method with regard to

technical parameters or processing software, differences in technique will continue to result in discrepancies in reported data.

A potentially more objective method for analyzing pediatric tumor rCBV compared to placement of an ROI is to utilize semi-automated methods which can generate more information regarding the tumor perfusion characteristics, such as entire tumor average rCBV or rCBV percentiles in addition to maximum rCBV. To our knowledge, this is the largest series of pediatric brain tumors analyzed with a semi-automated method for this purpose. The 95th percentile metric best reflects the manual rCBVmax as it evaluates the rCBV values in the 95th percentile of the tumor which is confirmed by the significant correlation between the two methods. Interestingly, the highest percentile metrics (95th and 90th) did not achieve significance compared to WHO grade, while the lower percentiles, average, and peak location were significant. This can be explained when looking at the whole-tumor histograms (Fig. 4), which show that, with the exception of ATRT, both low- and high-grade tumors have a similar histogram profile range, but that low-grade tumors, particularly pilocytics astrocytomas, have consistently lower percentile rCBV values. This explains our resulting low threshold of manual rCBV maximum of 1.38. Lev and Rosen [20] used a low rCBV threshold in adult gliomas of 1.5, which yielded 100 % sensitivity and 69 % specificity, which is similar to the threshold of Law et al. [1] at 1.75, also in adult gliomas, yielding 95 % sensitivity, 57.5 % specificity, and 79.3 % negative predictive value. Our findings in pediatric tumors are similar, where a low threshold of 1.38 yields 92 % sensitivity, 40 % specificity but high negative predictive value of 88 %. Similar to these results in adult gliomas, low rCBV thresholds are most useful in excluding high-grade pediatric neoplasms.

Finally, with the exception of a slightly higher sensitivity, manual rCBVmax threshold analysis has worse diagnostic accuracy in low- versus high-grade tumor discrimination compared to experienced pediatric neuroradiologists in our sample population. rCBV thresholds, however, may be of benefit as an adjunct to conventional imaging in challenging cases as represented by the 12 discordant cases between reviewers, where using a manual ROI rCBVmax threshold of 1.38 further improves the accuracy of low-high discrimination.

Only a few articles exist in the literature about the effects of dexamethasone treatment on MRI DSC perfusion of primary brain neoplasms, with none on pediatric brain tumors. Darpolor et al. [21] demonstrated a transient decrease in tumor rCBV on the third day of dexamethasone treatment which resolved on the fifth day in 13 gliosarcoma rat models. Conversely, Quarles et al. [22] showed an increase in rCBF on 15 gliosarcoma rats. Similarly, there is conflicting literature for the few articles on in vivo MRI DSC data on human brain tumors treated with dexamethasone. For example, Wilkinson et al. [23] demonstrated a significant reduction in rCBV in 17 patients treated with dexamethasone with contrast enhancing brain lesions of

heterogeneous etiology, of which 11 were grade IV gliomas. In contrast, both Armitage et al. [24] and Bastin et al. [25] demonstrated no significant change in rCBV for 8 and 10 patients, respectively, with glioblastomas treated with dexamethasone. However, Armitage et al. did demonstrate a significant reduction in permeability as measured by K(trans).

Assessing for changes in tumor perfusion, if any, from dexamethasone treatment is outside the scope of our research. However, our results demonstrate no significant differences in rCBVmax due to treatment with dexamethasone versus without for all included patients and between the highest-grade tumors, lowest-grade tumors, medulloblastoma, and pilocytic astrocytomas. These tumors were chosen due to their relatively larger representation within the entire cohort and are also representative of the most common grade IV and grade I pediatric brain tumors. The lack of any significant differences may be attributable to MRI evaluation within 2 days of the first dexamethasone dose, differences in dosing, and inherent differences in response of pediatric brain tumors to dexamethasone compared to adult tumors. Regardless, within our cohort, dexamethasone did not significantly alter our rCBV data.

Further research in the diagnostic evaluation of primary pediatric brain tumors and its perfusion characteristics should concentrate on specific pathologies which may have different molecular subtypes that correspond with different patient outcomes. A prime example is medulloblastoma, which has four known tumor subtypes that can range from good to poor prognosis [15]. Given that our medulloblastoma data has a broad range of low and high rCBVmax values, this may correlate with different molecular subtypes, and ultimately, patient outcome.

Limitations

The neuroradiologists evaluating the perfusion data were not blinded to the anatomic MRI sequences, some of which were highly suggestive of the tumor diagnosis. This was unavoidable because the anatomic images provide information integral in the assessment of the perfusion images (e.g., location of tumor, location of major vessels, etc.). This limitation is reasonable, however, because it reflects the process in which MR perfusion images are evaluated in clinical practice. Contrast infusion rate and peripheral intravenous catheter gauge are related issues that likely affect the quality of the perfusion study and are recognized challenges with performing DSC perfusion MRI on pediatric patients [10]. However, only one study out of the 65 identified by the search criteria was excluded for poor contrast medium bolus indicating high quality DSC perfusion MRI can be performed in pediatric brain tumor patients. This study was limited to primary pediatric brain tumors which had a surgically obtained WHO grade which resulted in exclusion of brain metastases and other primary brain tumors which did not have a proven WHO grade such as pontine gliomas.

Conclusions

Maximum rCBV obtained from manual ROI methods in DSC perfusion of pediatric primary brain tumors has significant positive correlation with WHO grade and is validated by our semiautomatic histogram data. However, considerable rCBV overlap exists between low- and high-grade pediatric brain tumors, particularly pilocytic astrocytomas and medulloblastomas, which limit the utility of rCBV quantitative thresholds between low- and high-grade tumors and is generally worse than the accuracy of the interpretation of an experienced pediatric neuroradiologist. In our sample, a quantitative rCBVmax threshold of 1.38 has a high negative predictive value for excluding high-grade neoplasms and may have a limited role as an adjunct in improving the accuracy in cases which present a diagnostic challenge.

Ethical standards and patient consent We declare that this manuscript does not contain clinical studies or identifiable patient data, and therefore, the Institutional Review Board of Indiana University waived consent.

Conflict of interest We declare that we have no conflict of interest.

References

1. Law M, Yang S, Wang H et al (2003) Glioma grading: sensitivity, specificity, and predictive values of perfusion MR imaging and proton MR spectroscopic imaging compared with conventional MR imaging. AJNR Am J Neuroradiol 24:1989–1998
2. Bulakbasi N, Kocaoglu M, Farzaliyev A et al (2005) Assessment of diagnostic accuracy of perfusion MR imaging in primary and metastatic solitary malignant brain tumors. AJNR Am J Neuroradiol 26: 2187–2199
3. Law M, Young R, Babb J et al (2007) Histogram analysis versus region of interest analysis of dynamic susceptibility contrast perfusion MR imaging data in the grading of cerebral gliomas. AJNR Am J Neuroradiol 28:761–766
4. Shin J, Lee H, Kwun B et al (2002) Using relative cerebral blood flow and volume to evaluate the histopathologic grade of cerebral gliomas: preliminary results. Am J Roentgenol 179:783–789
5. Law M, Young R, Babb J et al (2006) Comparing perfusion metrics obtained from a single compartment versus pharmacokinetic modeling methods using dynamic susceptibility contrast-enhanced perfusion MR imaging with glioma grade. AJNR Am J Neuroradiol 27:1975–1982
6. Fan G, Deng Q, Wu Z, Guo Q (2006) Usefulness of diffusion/ perfusion-weighted MRI in patients with non-enhancing supratentorial brain gliomas: a valuable tool to predict tumour grading? Br J Radiol 79:652–658
7. Morita N, Wang S, Chawla S et al (2010) Dynamic susceptibility contrast perfusion weighted imaging in grading of nonenhancing astrocytomas. J Magn Reson Imaging 32(4):803–808
8. Boxerman J, Schmainda K, Weisskoff R (2006) Relative cerebral blood volume maps corrected for contrast agent extravasation significantly correlate with glioma tumor grade, whereas uncorrected maps do not. AJNR Am J Neuroradiol 27:859–67
9. Ball W Jr, Holland S (2001) Perfusion imaging in the pediatric patient. Magn Reson Imaging Clin N Am 9:207–230
10. Yeom K, Mitchell L, Lober R et al (2014) Arterial spin-labeled perfusion of pediatric brain tumors. AJNR Am J Neuroradiol 35(2): 395–401. doi:10.3174/ajnr.A3670
11. Koeller K, Rushing E (2004) From the archives of the AFIP: pilocytic astrocytoma: radiologic-pathologic correlation. Radiographics 24: 1693–1708
12. Brat D, Scheithauer B, Fuller G, Tihan T (2007) Newly codified glial neoplasms of the 2007 WHO classification of tumours of the central nervous system: angiocentric glioma, pilomyxoid astrocytoma and pituicytoma. Brain Pathol 17:319–324
13. Lev M, Ozsunar Y, Henson J et al (2004) Glial tumor grading and outcome prediction using dynamic spin-echo MR susceptibility mapping compared with conventional contrast-enhanced MR: confounding effect of elevated rCBV of oligodendrogliomas. AJNR Am J Neuroradiol 25:214–221
14. Xu M, See S, Ng W et al (2005) Comparison of magnetic resonance spectroscopy and perfusion-weighted imaging in presurgical grading of oligodendroglial tumors. Neurosurgery 56:919–926
15. Kool M, Korshunov A, Remke M et al (2012) Molecular subgroups of medulloblastoma: an international meta-analysis of transcriptome, genetic aberrations, and clinical data of WNT, SHH, group 3, and group 4 medulloblastomas. Acta Neuropathol 123(4):473–84. doi: 10.1007/s00401-012-0958-8
16. Cha S (2006) Dynamic susceptibility-weighted contrast-enhanced perfusion MR imaging in pediatric patients. Neuroimaging Clin N Am 16(1):137–147
17. Grand S, Kremer S, Tropres I et al (2007) Perfusion-sensitive MRI of pilocytic astrocytomas: initial results. Neuroradiology 49(7):545–550
18. Yuh E, Barkovich A, Gupta N (2009) Imaging of ependymomas: MRI and CT. Childs Nerv Syst 25:1203–1213
19. Sentürk S, Oğuz K, Cila A (2009) Dynamic contrast enhanced susceptibility-weighted perfusion imaging of intracranial tumors: a study using a 3 T MR scanner. Diagn Interv Radiol 15:3–12
20. Lev MH, Rosen BR (1999) Clinical applications of intracranial perfusion MR imaging. Neuroimaging Clin N Am 9:309–331
21. Darpolor MM, Molthen RC, Schmainda KM (2011) Multimodality imaging of abnormal vascular perfusion and morphology in preclinical 9L gliosarcoma model. PLoS One 6(1):e16621
22. Quarles CC, Krouwer HG, Rand SD, Schmainda KM (2005) Dexamethasone normalizes brain tumor hemodynamics as indicated by dynamic susceptibility contrast MRI perfusion parameters. Technol Cancer Res Treat 4(3):245–9
23. Wilkinson ID, Jellineck DA, Levy D et al (2006) Dexamethasone and enhancing solitary cerebral mass lesions: alterations in perfusion and blood-tumor barrier kinetics shown by magnetic resonance imaging. Neurosurgery 58(4):640–6
24. Armitage PA, Schwindack C, Bastin ME, Whittle IR (2007) Quantitative assessment of intracranial tumor response to dexamethasone using diffusion, perfusion and permeability magnetic resonance imaging. Magn Reson Imaging 25(3):303–10
25. Bastin ME, Carpenter TK, Armitage PA et al (2006) Effects of dexamethasone on cerebral perfusion and water diffusion in patients with high-grade glioma. AJNR Am J Neuroradiol 27(2):402–8